




## RESEARCH ARTICLE

# The effect of imatinib therapy on tumour cycling hypoxia, tissue oxygenation and vascular reactivity [version 1; referees: 1 approved, 1 approved with reservations]

Miguel R. Gonçalves<sup>1</sup>, Sean Peter Johnson<sup>1,2</sup>, Rajiv Ramasawmy<sup>1</sup>, Mark F. Lythgoe<sup>1</sup>, R. Barbara Pedley<sup>2</sup>, Simon Walker-Samuel <sup>1</sup>

<sup>1</sup>Centre for Advanced Biomedical Imaging, Division of Medicine, University College London, London, WC1E 6DD, UK

<sup>2</sup>Cancer Institute, University College London, London, WC1E 6DD, UK

**v1** First published: 06 Jun 2017, 2:38 (doi: [10.12688/wellcomeopenres.11715.1](https://doi.org/10.12688/wellcomeopenres.11715.1))  
Latest published: 06 Jun 2017, 2:38 (doi: [10.12688/wellcomeopenres.11715.1](https://doi.org/10.12688/wellcomeopenres.11715.1))

## Abstract

**Background:** Several biomedical imaging techniques have recently been developed to probe hypoxia in tumours, including oxygen-enhanced (OE) and blood oxygen level-dependent (BOLD) magnetic resonance imaging (MRI). These techniques have strong potential for measuring both chronic and transient (cycling) changes in hypoxia, and to assess response to vascular-targeting therapies in the clinic.



**Methods:** In this study, we investigated the use of BOLD and OE-MRI to assess changes in cycling hypoxia, tissue oxygenation and vascular reactivity to hyperoxic gas challenges, in mouse models of colorectal therapy, following treatment with the PDGF-receptor inhibitor, imatinib mesylate (Glivec).

**Results:** Whilst no changes were observed in imaging biomarkers of cycling hypoxia (from BOLD) or chronic hypoxia (from OE-MRI), the BOLD response to carbogen-breathing became significantly more positive in some tumour regions and more negative in other regions, thereby increasing overall heterogeneity.

**Conclusions:** Imatinib did not affect the magnitude of cycling hypoxia or OE-MRI signal, but increased the heterogeneity of the spatial distribution of BOLD MRI changes in response to gas challenges.

## Open Peer Review

Referee Status:  

	Invited Referees	
	1	2
<b>version 1</b> published 06 Jun 2017	 report	 report
1	<b>Mark W. Dewhirst</b> , Duke University, USA <b>Ashlyn Rickard</b> , Duke University, USA <b>Xiaojie Zhang</b> , Duke University, USA	
2	<b>Bernard Gallez</b> , Universite catholique de Louvain, Belgium	

## Discuss this article

Comments (0)

**Corresponding author:** Simon Walker-Samuel ([simon.walkersamuel@ucl.ac.uk](mailto:simon.walkersamuel@ucl.ac.uk))

**Competing interests:** No competing interests were disclosed.

**How to cite this article:** Gonçalves MR, Johnson SP, Ramasawmy R *et al.* **The effect of imatinib therapy on tumour cycling hypoxia, tissue oxygenation and vascular reactivity [version 1; referees: 1 approved, 1 approved with reservations]** Wellcome Open Research 2017, 2:38 (doi: [10.12688/wellcomeopenres.11715.1](https://doi.org/10.12688/wellcomeopenres.11715.1))

**Copyright:** © 2017 Gonçalves MR *et al.* This is an open access article distributed under the terms of the [Creative Commons Attribution Licence](https://creativecommons.org/licenses/by/4.0/), which permits unrestricted use, distribution, and reproduction in any medium, provided the original work is properly cited.

**Grant information:** This work was carried out as part of King's College London and UCL Comprehensive Cancer Imaging Centre, and The Institute of Cancer Research Cancer Imaging Centre, CR-UK & EPSRC, in association with the Medical Research Council (MRC), Department of Health and British Heart Foundation (England) (C1519/A10331, C1519/A16463). RBP receives funding from the Medical Research Funding DPFS grant (MRC G100149). MFL receives funding from MRC (MR/J013110/1); the National Centre for the Replacement, Reduction and Refinement of Animal in Research (NC3Rs); UK Regenerative Medicine Platform Safety Hub (MRC: MR/K026739/1). SW-S is a Wellcome Trust Senior Research Fellow (WT100247MA).

*The funders had no role in study design, data collection and analysis, decision to publish, or preparation of the manuscript.*

**First published:** 06 Jun 2017, 2:38 (doi: [10.12688/wellcomeopenres.11715.1](https://doi.org/10.12688/wellcomeopenres.11715.1))

## Introduction

Changes in tumour blood oxygen saturation, blood flow and tissue oxygen concentration can each be detected noninvasively via recent advances in magnetic resonance imaging (MRI). In particular, blood oxygen level dependent (BOLD) MRI allows changes in tumour deoxyhaemoglobin concentration to be detected<sup>1,2</sup> and oxygen-enhanced (OE) MRI uses the change in longitudinal relaxation time to detect changes in oxygen concentration in tissue, resulting from inhalation of a hyperoxic gas<sup>2,3</sup>.

Using these biomedical techniques, alongside others, it has been found that numerous solid tumours exhibit cyclical variations in blood flow and/or oxygenation, resulting in cycling hypoxia in tumour tissue, with a period of minutes to hours or even days<sup>4–8</sup>. This effect has been detected non-invasively with biomedical imaging in a number of studies<sup>6,9–14</sup>, but remains relatively under-studied<sup>15</sup>.

Both cycling and chronic hypoxia can impact on treatment efficacy. Cycling hypoxia has been found to contribute to therapeutic resistance by limiting tumour drug delivery<sup>16</sup> or, alongside chronic hypoxia, by lowering oxygen concentration (which can impact on response to both radiotherapy and chemotherapy<sup>17</sup>). A better understanding of the effects of both cycling and chronic hypoxia on treatment efficacy and drug delivery is critically needed. Moreover, the use of therapeutic agents with previously established and well-understood mechanisms of action can provide novel insights into the mechanisms underpinning cycling hypoxia.

We therefore sought to investigate the effect of treatment with imatinib mesylate, a tyrosine-kinase inhibitor of platelet-derived growth factor (PDGF) receptor<sup>18–20</sup> on cycling and chronic hypoxia. We hypothesised that potential vascular normalisation induced by imatinib<sup>21</sup> would alleviate hypoxia and decrease the occurrence of blood flow fluctuations associated with cycling hypoxia, via remodelling of the vasculature, and with a similar effect on chronic hypoxia. PDGF has an important role in angiogenesis<sup>22–25</sup> and imatinib has been found to reduce microvascular density<sup>26–29</sup>, reduce pericyte coverage<sup>30,31</sup>, decrease interstitial fluid pressure (IFP) in human xenograft models of lung (A549) and colorectal carcinoma<sup>27,32</sup> and improve the uptake of chemotherapeutic and radioimmunotherapeutic agents<sup>26,29,32–34</sup>. If these changes impact on cycling hypoxia, this would allow the development of non-invasive imaging biomarkers of early response to antiangiogenic therapy, for use in the clinic<sup>35</sup>.

In this study, BOLD and OE-MRI were used to assess changes in cycling hypoxia and oxygen delivery in colorectal tumour xenograft models (LS174T), during treatment with imatinib. Cycling hypoxia was assessed prior to and following imatinib therapy, using an hour-long, dynamic measurement that was sensitive to changes in blood oxygen concentration. We have previously detected and characterised cycling hypoxia in these models, detecting cyclical fluctuations with a period of approximately 3 cycles/hour<sup>36</sup>. BOLD and OE-MRI changes in response to hyperoxia and hypercapnia challenges were also assessed, and compared with gold-standard histological measures.

Our linked hypotheses to evaluate in this study were that imatinib therapy would: 1) reduce hypoxia, which would be detectable through BOLD and OE-MRI measurements; 2) reduce the amplitude and prevalence of cycling hypoxia via a reduction in blood volume and improvement in flow, due to pruning of immature vessels; and 3) increase responsiveness to gas challenges through similar mechanisms.

## Materials and methods

### Animal models

All *in vivo* experiments were performed in accordance with the UK Home Office Animals Scientific Procedures Act, 1986 and United Kingdom Coordinating Committee on Cancer Research (UKCCCR) guidelines<sup>37</sup>, and with the approval of the University College London Animal Ethics Committee. Female, CD1 nude mice (6–9 weeks old) were sourced from Harlan (UK) and were housed in groups of 5 in isolated ventilated cages (IVCs) containing environmental stimulation. Mice had access to food and water *ad libitum*.

LS174T human colorectal adenocarcinoma cells (provided by Prof. Pedley, UCL Cancer Institute) were grown for 2 weeks prior to injection in complete media (Minimum Essential Medium Eagle with L-Glutamine (EMEM) (Lonza, Belgium) + 10% fetal bovine serum (Invitrogen, UK)) in a ratio 1:20 (v/v) and incubated at 37°C and 5% CO<sub>2</sub>. To prepare for injection, cells were washed with DPBS and detached with trypsin-EDTA (7–8 min, 37°C, 5% CO<sub>2</sub>). 5 × 10<sup>6</sup> cells were injected subcutaneously into the left flank the mice.

### Imatinib therapy protocol

Imatinib (Glivec, Novartis Pharma GmbH, Germany) was administered by oral gavage (100 mg kg<sup>-1</sup> day<sup>-1</sup>) immediately after each animal's first MRI scan (day 0), and then daily for five consecutive days (*n* = 10). Animals in the control group were treated with saline (*n* = 9). Daily calliper measurements were taken to assess tumour growth rate. Tumour volume (*V*) was estimated according to:  $V = (\pi/6) \times a \times b^2$ , where *a* is the longest diameter of the tumour, and *b* is the diameter orthogonal to *a*.

### *In vivo* MRI

All MRI scans were performed on a 9.4 T VNMRS Varian scanner (20 cm bore) using a 39 mm birdcage coil (Rapid MR International, Columbus, Ohio). Prior to MR imaging, anaesthesia was induced in mice with 5% isoflurane in medical air (78% N<sub>2</sub> + 21% O<sub>2</sub> + traces of Ar, CO<sub>2</sub>, H<sub>2</sub>, water vapour and others) and subsequently maintained in the scanner with 1.25–1.5% isoflurane in medical air, oxygen, or other gas mixtures, at 1 L/minute, administered via a nose cone. During scanning, core temperature was measured using a rectal thermometer and maintained using a warm air blower and warm water pipes. Respiratory rate was also monitored using bellows (SA Instruments, Stony Brook, US) and maintained at 60 – 90 breaths per minute by adjusting isoflurane concentration. Tumours were set in dental paste (Charmflex, Dentkist, South Korea) throughout scanning, to eliminate motion artefacts.

Baseline MRI scans were performed following approximately two weeks of tumour growth (day 0). Following pilot scans and shimming, three sets of data were acquired. The first acquisition was a 60-minute, dynamic BOLD scan, acquired using a gradient echo multi-slice sequence, which was used to detect periodic changes in deoxyhaemoglobin concentration (see post-processing below). Sequence parameters included: repetition time (TR), 59.62 ms; 5 echoes; first echo time (TE), 2 ms; echo spacing, 2 ms; in-plane field of view, 20×20 mm<sup>2</sup>; matrix size, 64×64; slice thickness, 1.5 mm; 5 slices; 3.8 s per image.

The second acquisition was a 40-minute BOLD ‘gas challenge’ scan, during which different gas mixtures were administered in 10-minute intervals: medical air (including 20% O<sub>2</sub>, 2% CO<sub>2</sub>), carbogen (95% O<sub>2</sub>, 5% CO<sub>2</sub>), medical air, medical air + 5% CO<sub>2</sub>. The same sequence parameters were used as in the first BOLD scan, but with fewer acquisitions. Changes in signal intensity (SI) and  $\Delta R_2^*$  relative to air-breathing phases were measured.

The final acquisition was a Look-Locker segmented Inversion Recovery sequence, from which two  $R_1 (=1/T_1)$  maps were calculated, one during air breathing and another during carbogen breathing. Look-Locker sequence parameters included: TR, 10 s; 50 inversion times (TI); TI spacing, 110 ms; TR<sub>ref</sub>, 2.3 ms; TE, 1.18 ms; in-plane field of view 20×20 mm<sup>2</sup>; matrix size, 128×128; slice thickness, 1.5 mm; 5 slices; flip angle, 8°.

The complete MRI protocol was repeated at days 3 and 5 of the study.

### MRI data analysis

Four different spatial maps were calculated: 1) standard deviation maps of spontaneous  $R_2^*$  fluctuations ( $R_2^*$  SD maps); 2)  $R_2^*$  maps of the difference between carbogen and air breathing ( $\Delta R_2^*$ ); 3)  $R_1$  maps of the difference between carbogen and air breathing ( $\Delta R_1$ ); 4) signal intensity (SI) maps of the difference between hypercapnia and air breathing ( $\Delta SI$ ).

Maps of  $R_2^*$  SD were acquired in order to estimate the percentage of voxels spontaneously fluctuating above the background noise uncertainty, and their respective amplitude. A Bayesian maximum a posteriori (MAP) approach was used to identify fluctuations above the background noise<sup>38</sup>.

Gas challenge time courses were used to create voxel-wise maps of vessel functionality carbogen (VF) and vessel maturation (VD)<sup>11</sup>. VF maps were created from the difference between the mean  $R_2^*$  values during carbogen breathing and air breathing; VD maps were created from the difference between the mean signal intensity (SI) values during hypercapnia and air breathing:

$$VF = \Delta R_{2Carb}^* = \overline{R_2^*(carbogen)} - \overline{R_2^*(air)}$$

$$VD = \Delta SI_{CO_2} = \overline{SI(air + 5\% CO_2)} - \overline{SI(air)} . \quad (1)$$

Maps of the change in  $R_1$  ( $\Delta R_1$ ) between carbogen and air breathing phases were calculated to estimate tissue oxygenation changes.

Paramagnetic dissolved molecular oxygen accelerates  $T_1$  relaxation through dipole-dipole interactions between the water protons and the molecular oxygen<sup>39</sup>. Voxel-wise  $\Delta R_1$  maps were calculated as:

$$\Delta R_1 = \frac{1}{T_{1Carb}} - \frac{1}{T_{1Air}} , \quad (2)$$

An increase in tissue oxygenation upon carbogen breathing was expected to produce a positive  $\Delta R_1$ . The percentage of positive or negative carbogen-responsive voxels and its mean  $\Delta R_1$  value were computed for all treated tumours ( $n = 8$ ) and 3 control tumours.  $\Delta R_1$  maps were resampled to a matrix size of 64×64 in order to perform a correlation analysis with  $\Delta R_2^*$  maps to allow comparison of tissue oxygenation and blood oxygenation estimates in treated tumours. The magnitude values of individual voxels in both maps were plotted against each other (only supra-threshold voxels in  $\Delta R_2^*$  maps were considered). One plot was created for each day of MRI scanning. In each plot, voxels of all respective tumours were grouped ( $n = 8$ ). The percentage of voxels exhibiting positive or negative  $\Delta SI$  responses and their respective mean magnitude values were computed.

### Histological assessment

Multifluorescence histochemical labelling was undertaken on 10µm-thick frozen sections of tumour tissue. Staining for vascular perfusion was achieved via intravenous injection of Hoechst 33342 (Cambridge Bioscience, UK) at 12.5 mg/kg, one minute before sacrificing the animal by cervical dislocation. Endothelial cells were stained with a rat monoclonal antibody against CD31 (Abcam, UK, ab56299), revealed with Alexa Fluor-488 (Life Technologies, UK).

Pericytes express a number of markers of differentiation and, consequently, no single marker has the ability to identify all pericytes<sup>40</sup>. In this study, two markers were therefore used:  $\alpha$ -smooth muscle actin ( $\alpha$ -SMA) and NG2 chondroitin sulfate proteoglycan. The expression of  $\alpha$ -SMA occurs in most perivascular cells (composed of pericytes and vascular smooth muscle cells), whereas NG2 is expressed on arteriolar perivascular cells and capillary pericytes but not on venular pericytes<sup>40,41</sup>. Since the vasculature of LS174T tumours is predominantly composed of capillaries, both antibodies exclusively stain pericytes in this tumour type. Moreover, the expression of  $\alpha$ -SMA is possibly dependent on endothelial release of transforming growth factor- $\beta$  (TGF- $\beta$ ), whereas differentiation into NG2-positive pericytes is independent of TGF- $\beta$ <sup>42</sup>. Pericyte staining was therefore undertaken with both mouse monoclonal anti- $\alpha$ -SMA (Sigma-Aldrich, UK, A5228) labelled with Alexa Fluor 546 (Life Technologies, UK, A20183) and rabbit polyclonal anti-NG2 antibody (Millipore, UK, 05-710) labelled with Alexa Fluor-488 (Life Technologies, UK, A20181).

Hypoxic regions were detected via intraperitoneal injection (60 mg/kg) of the hypoxia marker pimonidazole (Hypoxyprobe, US) 30 minutes before sacrificing the animal by cervical dislocation, followed by *ex vivo* staining using a rabbit polyclonal anti-pimonidazole (Hypoxyprobe, US), labelled with Alexa Fluor-488 (Life Technologies, UK). Additionally, haematoxylin and eosin (H&E) staining was performed in immediately adjacent frozen sections to assess tumour morphology.

Fluorescence images were acquired using an Axio Imager microscope (Carl Zeiss, UK), equipped with an AxioCam digital colour camera. H&E images were collected on a bright-field Zeiss Axioskop2 microscope (Carl Zeiss, UK). Both microscopes were fitted with a motorized stage and used AxioVision software (Carl Zeiss, UK); acquisition magnification was 10x objective.

Quantification of immunofluorescence was performed in Matlab (MathWorks, MA, US). Regions of interest (ROIs) were drawn around the total area of the tumour and images were thresholded to exclude background fluorescence signal. Tumour coverage of Hoechst 33342 and each of the four fluorescent markers was calculated as the ratio between fluorescent pixels and the total number of pixels within the ROI. Additionally, the percentage of capillaries (CD31) covered with pericytes ( $\alpha$ -SMA or NG2) was calculated to assess vascular maturation.

### Statistical analysis

Differences in the growth rate between treated and control tumours (calculated by MRI or calliper measurements) were assessed with a Mann-Whitney *U*-test on each individual day. The same test was used for assessing differences between treated and control tumours regarding quantitative distributions of histological fluorescence markers.

In order to assess the effect of imatinib administration on tumour MRI parameter estimates, a longitudinal assessment of individual tumours (i.e., throughout the study days) was undertaken. A one-way ANOVA followed by Holm-Šidák's multiple comparisons test was used to assess significant differences between days 0, 3 and 5 in treated tumours. The same test was used separately in the control group. This was performed for  $R_2^*$  spontaneous fluctuations,  $R_2^*$  response to carbogen,  $R_1$  response to carbogen and SI response

to hypercapnia. Voxel-wise correlation between  $\Delta R_2^*$  and  $\Delta R_1$  responses to carbogen breathing was assessed with Pearson's linear correlation.

## Results

### Assessment of tumour growth rate

Administration of imatinib did not significantly affect the growth rate of LS174T tumours, as assessed by both MRI and calliper measurements (see Figure 1). This is consistent with previous studies in the same tumour type<sup>18</sup>, although changes were observed on histology. In the imatinib-treated group, one mouse was euthanized prior to therapy due to tumour ulceration.

### Effect of imatinib on BOLD MRI measurements of cycling hypoxia

Maps showing cyclical fluctuations in an LS174T tumour, and associated BOLD MRI  $R_2^*$  time courses, are shown in Figure 2. As found in our previous study in this tumour type, fluctuations exhibited a period of approximately 3 cycles/hour<sup>36</sup>. Imatinib therapy did not cause a significant change ( $P>0.05$ ) in the number of voxels exhibiting cyclical  $R_2^*$  fluctuations, nor their magnitude, at any point throughout the duration of the study. The data from one control tumour were unevaluable due to extensive susceptibility artefacts, and were excluded from further analysis.

### BOLD MRI measurements during hyperoxia gas challenge

Figure 3 shows the  $R_2^*$  response to a hyperoxia challenge (carbogen), assessed with BOLD MRI, in an example tumour. The percentage of voxels exhibiting positive ( $+\Delta R_2^*$ , implying an increase in deoxyhaemoglobin) or negative ( $-\Delta R_2^*$ , implying a decrease in deoxyhaemoglobin) responses did not change significantly throughout the study, either in treated or control groups (Figure 3B), nor did the magnitude of  $R_2^*$  responses (Figure 3C).

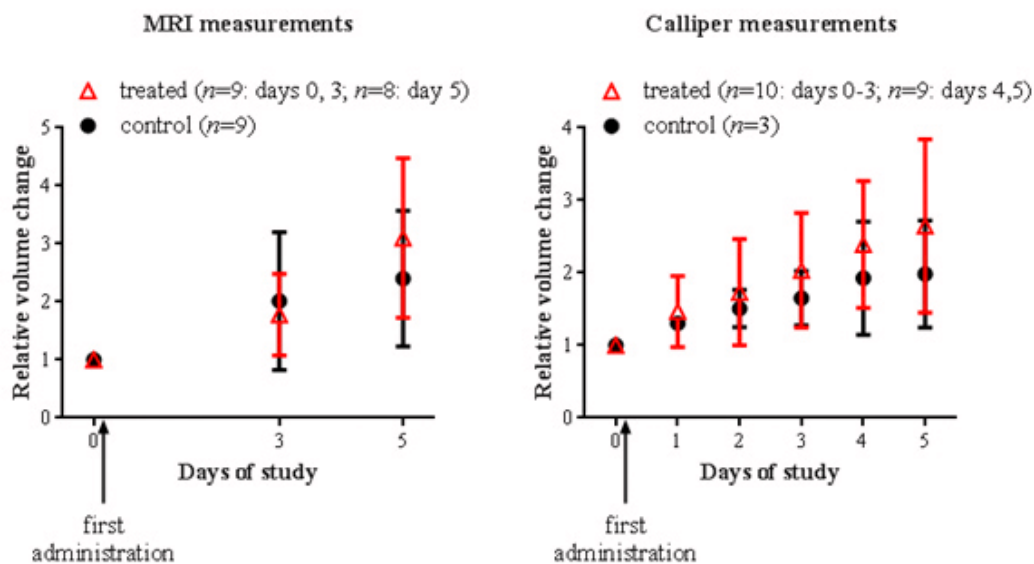


**Figure 1.** Tumour growth in treated (imatinib) and control (saline) tumours, assessed with MRI (left) and calliper (right) measurements. The first dose of Imatinib or saline was administered to the mice immediately after the baseline scan, and a further four doses were given, once a day. No significant differences in growth rate between the groups were identified (Mann-Whitney *U*-test). Data are mean  $\pm$  SD.

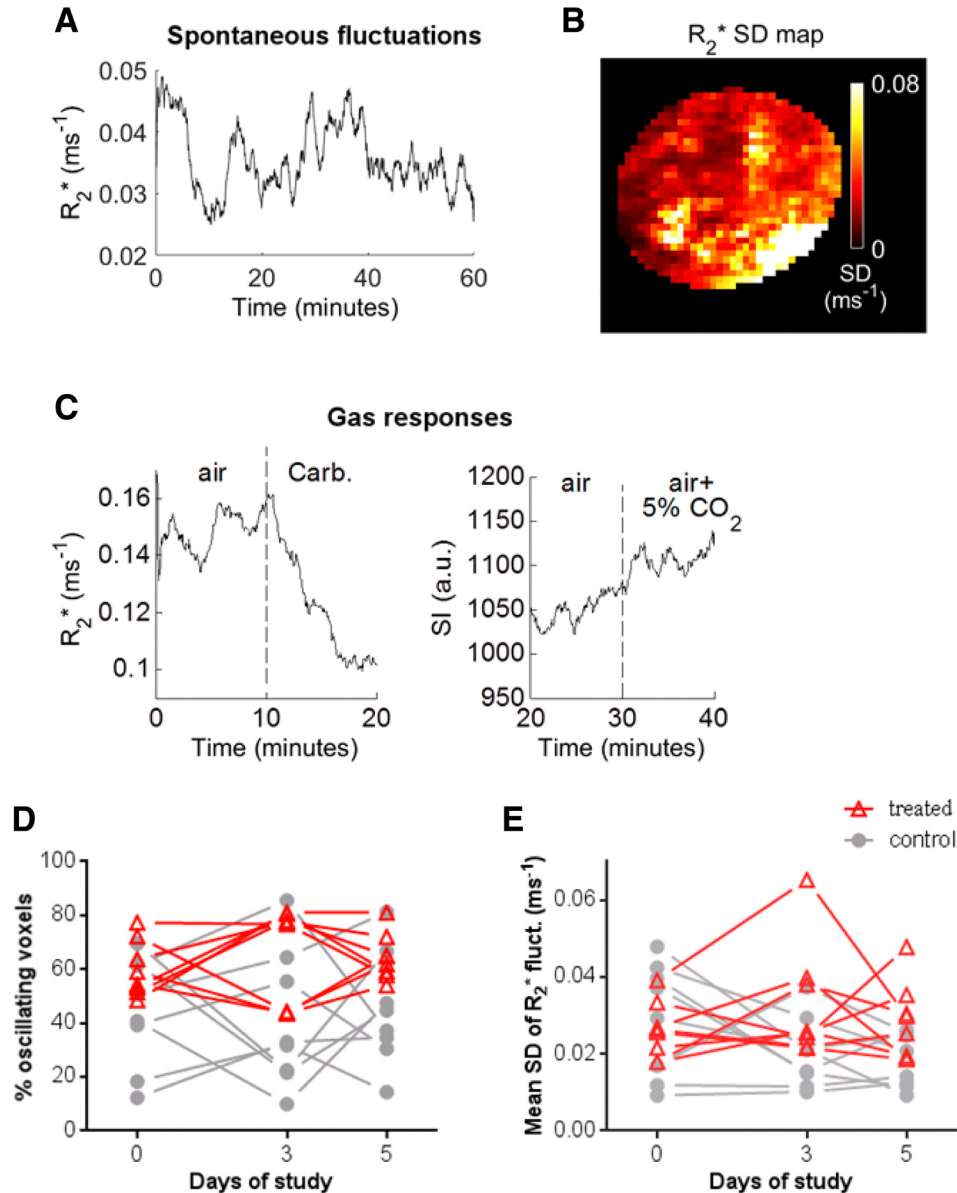


**Figure 2. Spontaneous fluctuations in tumour blood oxygenation, measured with BOLD-MRI.** **A**)  $R_2^*$  time course in an example voxel exhibiting spontaneous fluctuations. **B**) An example  $R_2^*$  standard deviation (SD) map, showing the location of spontaneous fluctuations within a slice through an LS174T tumour. **C**) Graphs showing the change in  $R_2^*$  in example voxels, during air breathing followed by carbogen (carb, 95%  $O_2$  / 5%  $CO_2$ ) breathing, and the change in signal intensity during air breathing followed by to air+5%  $CO_2$  breathing. **D**) The percentage of tumour voxels, across the whole group of mice, that exhibited statistically significant spontaneous  $R_2^*$  fluctuations and the corresponding standard deviation of such variations. No significant differences in these measures were found in the treated (imatinib,  $n = 8$ ) or control (saline,  $n = 8$ ) groups throughout the study days (one-way ANOVA followed by Holm-Šidák's multiple comparisons test).

However, an interesting effect was observed in the BOLD response to hyperoxia by the treated group at day 5, where either positive or negative responses were of larger magnitude than at days 0 and 3 (Figure 3C). This observation led to the investigation of the heterogeneity in the tumour response via measurements of standard deviation (SD) of  $\Delta R_2^*$  values in each tumour. SD values of  $\Delta R_2^*$  were found to significantly increase in the treated group at day 5, but not in the control group, confirming an increase in

the response heterogeneity throughout the tumour due to imatinib (Figure 3D).

BOLD MRI measurements during hypercapnia gas challenge Figure 4 shows the tumour response to hypercapnia challenge. The percentage of responsive voxels (both positive and negative) and their corresponding magnitudes were not significantly different between study days in treated or control groups.

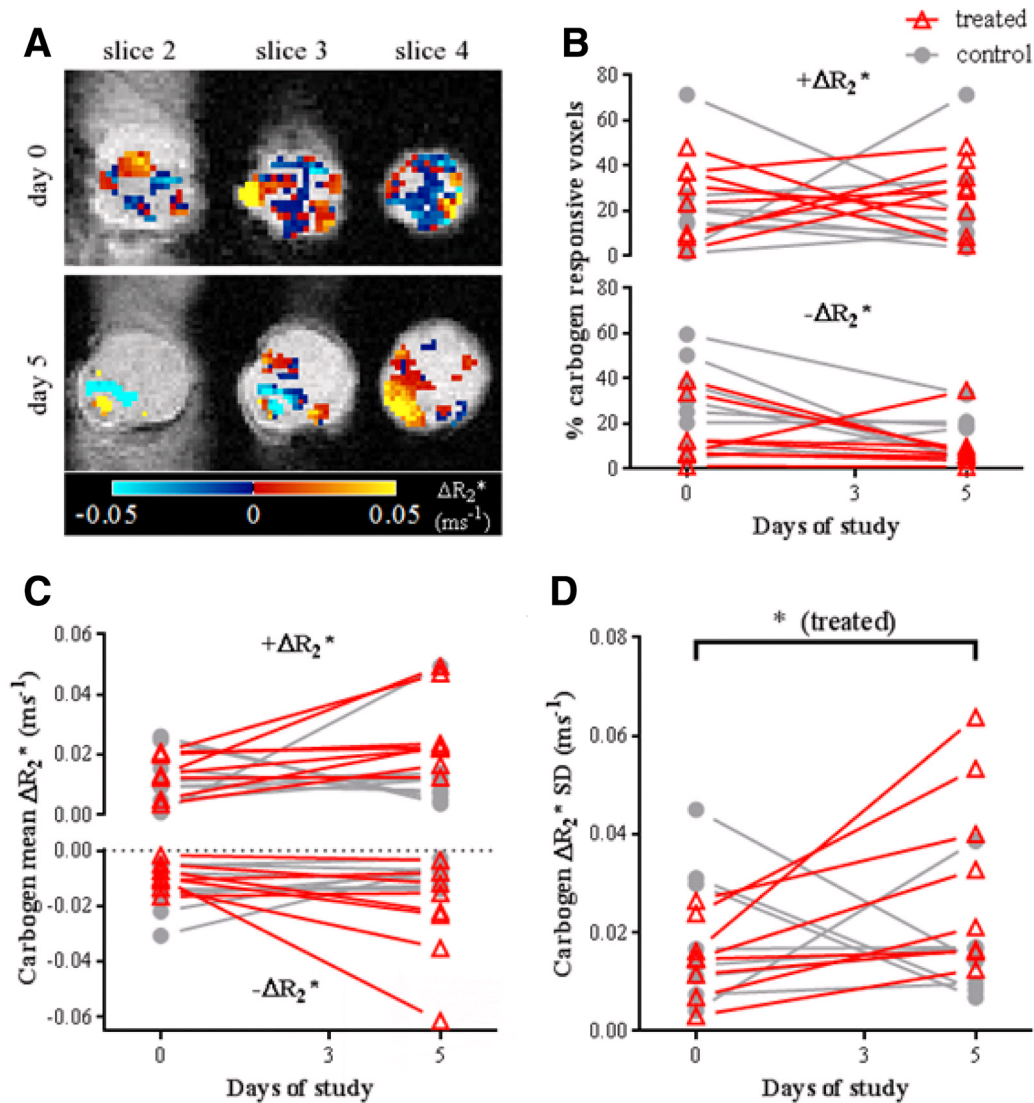


**Figure 3. Tumour  $R_2^*$  response to hyperoxia (carbogen) challenge at baseline (day 0) and day 5 of Imatinib therapy.** Statistical significance throughout the study in treated (imatinib,  $n = 8$ ) or control (saline,  $n = 8$ ) groups was tested with a one-way ANOVA followed by Holm-Šidák's multiple comparisons test. **A**) A representative dataset showing an increase in the heterogeneity of carbogen response caused by imatinib therapy, between days 0 and 5. **B**) A ladder plot showing the percentage of tumour voxels showing a significantly positive or negative  $R_2^*$  response to carbogen. **C**) Ladder plot showing the corresponding mean  $\Delta R_2^*$  values for each treated or control tumour. **D**) The standard deviation of the magnitude values represented in **C**, depicting a significant increase in the heterogeneity of the carbogen response between days 0 and 5 in the treated group, but not in the control group. \* $P < 0.05$ .

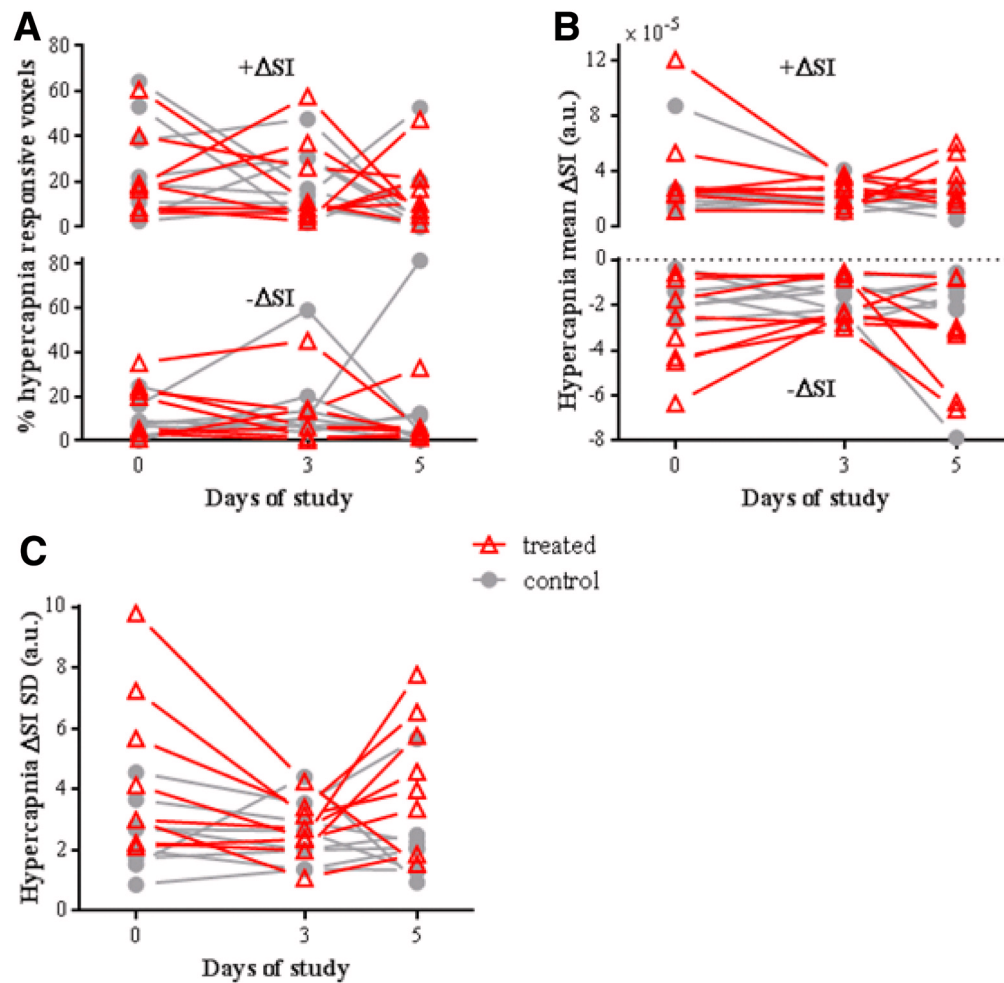
### OE-MRI measurements

Figure 5 shows OE-MRI measurements in an example tumour, measured using the change in  $R_1$  following a hyperoxia (carbogen) challenge.  $\Delta R_1$  was not significantly different between study days, in either treated or control groups (Figure 5B).

### Immunohistochemistry

Histological data from two treated tumours were unevaluable due to sectioning artefacts, leaving seven treated tumours available for histological assessment. The histological sample size of the

control group was: perfusion ( $n=5$ ), hypoxia ( $n=5$ ), endothelial cells ( $n=10$ ), pericytes ( $\alpha$ -SMA,  $n=10$ ), pericytes (NG2,  $n=6$ ), pericyte ( $\alpha$ -SMA) coverage of blood vessels ( $n=10$ ), and pericyte (NG2) coverage of blood vessels ( $n=6$ ) (Figure 6A-C). Imatinib-treated tumours exhibited a significantly reduced number of capillaries covered with NG2-stained pericytes, relative to control tumours ( $P < 0.01$ ). However, no difference was found in the percentage of capillaries covered with  $\alpha$ -SMA-stained pericytes between treated and control groups. No significant differences were observed in markers of perfusion, hypoxia, vascular endothelial cells or



**Figure 4. Tumour signal intensity (SI) response to air + 5% CO<sub>2</sub> breathing challenge (hypercapnia) at days 0 (baseline), 3 and 5. A)** Ladder plot showing the percentage of tumour voxels showing a positive (+ $\Delta$ SI) or negative (- $\Delta$ SI) response to hypercapnia. **B)** Corresponding mean  $\Delta$ SI values for each treated or control tumour. **C)** Standard deviation of the magnitude values represented in **B**. No significant differences were observed throughout the study in the treated or control groups (one-way ANOVA followed by Holm-Šidák's multiple comparisons test).

pericytes (neither  $\alpha$ -SMA nor NG2). Imatinib-treated tumours also exhibited hyperdilated blood vessels, potentially due to a loss of structural support from the decreased pericyte coverage (NG2). This was not found in untreated tumours. Of note was that the method used to quantify tumour coverage of histological measures did not take into account the morphological changes exhibited by the vasculature. The fact that some capillaries were larger in treated tumours could also mean there were fewer of them in the corresponding area, although we found no evidence for overall differing microvascular density between treated and control groups.

## Discussion

The effect of treatment with imatinib mesylate, a tyrosine-kinase inhibitor of PDGF receptor, on spontaneous fluctuations in tumour blood oxygenation and responsiveness to vasoactive gas challenges, was investigated here, using blood oxygen level-dependent (BOLD) and oxygen-enhanced (OE) MRI. Our starting

hypothesis was that vascular normalisation induced by imatinib would reduce vascular fluctuations (via a reduction in interstitial fluid pressure) and enhance the response to hyperoxic gas challenges<sup>17,22</sup>.

## Effect of imatinib therapy on histological measures

Quantification of histological data revealed that the regime of drug administration used (100 mg kg<sup>-1</sup>, once per day for 5 consecutive days) did not appear to induce functional normalisation of the tumour microvasculature. Perfusion and hypoxia were not significantly different from control tumours. This result could possibly be due to the relatively short therapy window (5 days, compared with 7 days in previous studies<sup>26,32</sup>) and/or that therapy was not fractionated (the half-life of imatinib is approximately 4 hours in mice<sup>43</sup>, meaning a fractionated dose can be more effective<sup>32</sup>). However, fractionated dosing would have been challenging to implement due to the timing of MRI scans.



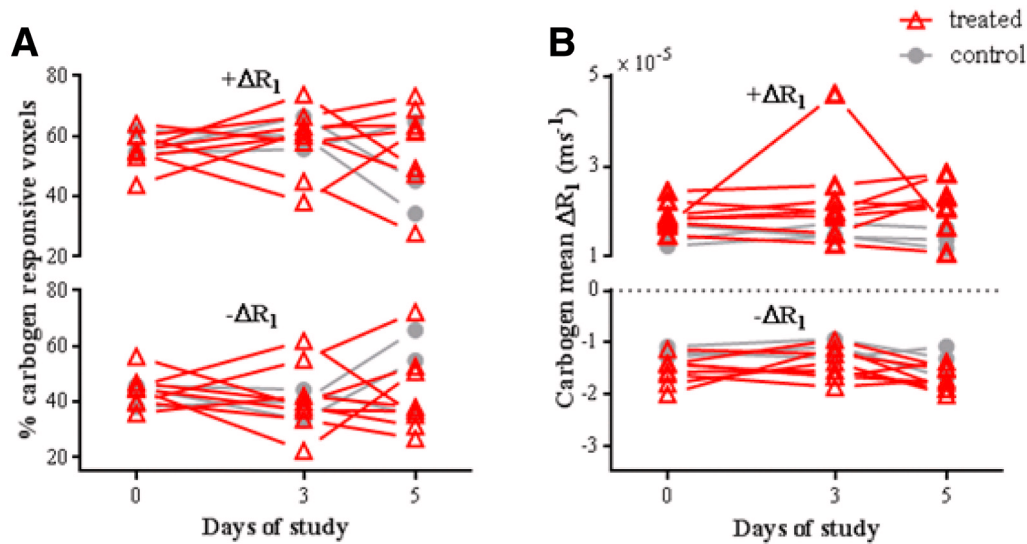


**Figure 5.** Tumour  $R_1$  response to the carbogen challenge, assessed using OE-MRI, at days 0, 3 and 5 in treated (imatinib,  $n = 8$ ) and control (saline,  $n = 3$ ) groups. **A)** Ladder plot showing the percentage of tumour voxels that displayed a positive or negative  $R_1$  response. **B)** Corresponding mean  $\Delta R_1$  values for each treated or control tumour. No significant differences were observed throughout the study in the treated or control groups (one-way ANOVA followed by Holm-Šidák's multiple comparisons test).

In contrast, vascular coverage of pericytes (expressing NG2) was found to decrease with therapy, which is consistent with inhibition of the PDGF pathway by imatinib<sup>19</sup>. Disruption of the pericyte-capillary contact resulted in blood vessel hyperdilation (Figure 6). This effect was previously observed following treatment with a PDGF-R inhibitor, where Song *et al.*<sup>42</sup> concluded that tumour pericytes, albeit less abundant or more loosely attached relative to normal vasculature, still played an important role in maintaining vascular integrity and function.

Decreased pericyte coverage has been proposed to increase leakage into the extravascular space<sup>44</sup> and, consequently, are associated with an increase interstitial fluid pressure (IFP). However, PDGF is a critical regulator of IFP<sup>33,34,45</sup> and imatinib-mediated inhibition of its receptor has previously been shown to decrease IFP and hypoxia in LS174T tumours<sup>32</sup>. No differences in hypoxia caused by imatinib were observed in this study, and the reasons for this disparity are unclear, but might be the result of these two antagonistic effects cancelling each other.

#### Effect of imatinib therapy on spontaneous $R_2^*$ fluctuations measured with BOLD MRI

Imatinib therapy did not affect the percentage of oscillating voxels or the amplitude of  $R_2^*$  fluctuations, which might be expected given the limited evidence of vascular normalisation found in histological measurements. However, even with confirmed pericyte detachment observed following therapy, spontaneous  $R_2^*$  fluctuations were still present. This suggests that pericytes have a minor role in the production of spontaneous fluctuations. Indeed, other studies have suggested that raised interstitial fluid pressure is responsible for the phenomenon, which can be caused by the periodic occlusion of vessels<sup>46</sup> or systemic fluctuations in blood

flow<sup>47</sup>. Imatinib therapy did not affect the percentage of oscillating voxels or the amplitude of  $R_2^*$  fluctuations, which might be expected given the limited evidence of vascular normalisation found in histological measurements. However, even with confirmed pericyte detachment observed following therapy, spontaneous  $R_2^*$  fluctuations were still present. This suggests that pericytes have a minor role in the production of spontaneous fluctuations. Indeed, other studies have suggested that raised interstitial fluid pressure is responsible for the phenomenon, which can be caused by the periodic occlusion of vessels<sup>46</sup> or systemic fluctuations in blood flow<sup>47</sup>.

#### BOLD and OE-MRI measurements in response to hyperoxia and hypercapnia

Imatinib-treated tumours displayed interesting effects on BOLD measurements during gas challenges, and which are not straightforward to interpret. An increase in the magnitude of  $\Delta R_2^*$  values (both positive and negative), measured during carbogen breathing, was observed at day 5 of the study. Vessel hyperdilation was evident in histological measures, and this increased blood volume could increase the tumour's capacity for oxygen transport, resulting in a more negative  $\Delta R_2^*$ . In turn, a greater response to the challenge could increase the potential for vascular steal effects from the nearby vasculature, causing a more positive  $\Delta R_2^*$ . A combination of these effects could therefore explain the increased BOLD response to carbogen.

Imatinib did not cause a significant change in the OE-MRI response to carbogen challenge throughout the study. Additionally, correlation between carbogen  $\Delta R_2^*$  and  $\Delta R_1$  revealed a weak correspondence. This contrasts with the study by O'Connor *et al.*<sup>48</sup>, in which  $R_2^*$  and  $R_1$  responses to carbogen and oxygen inhalation in patients

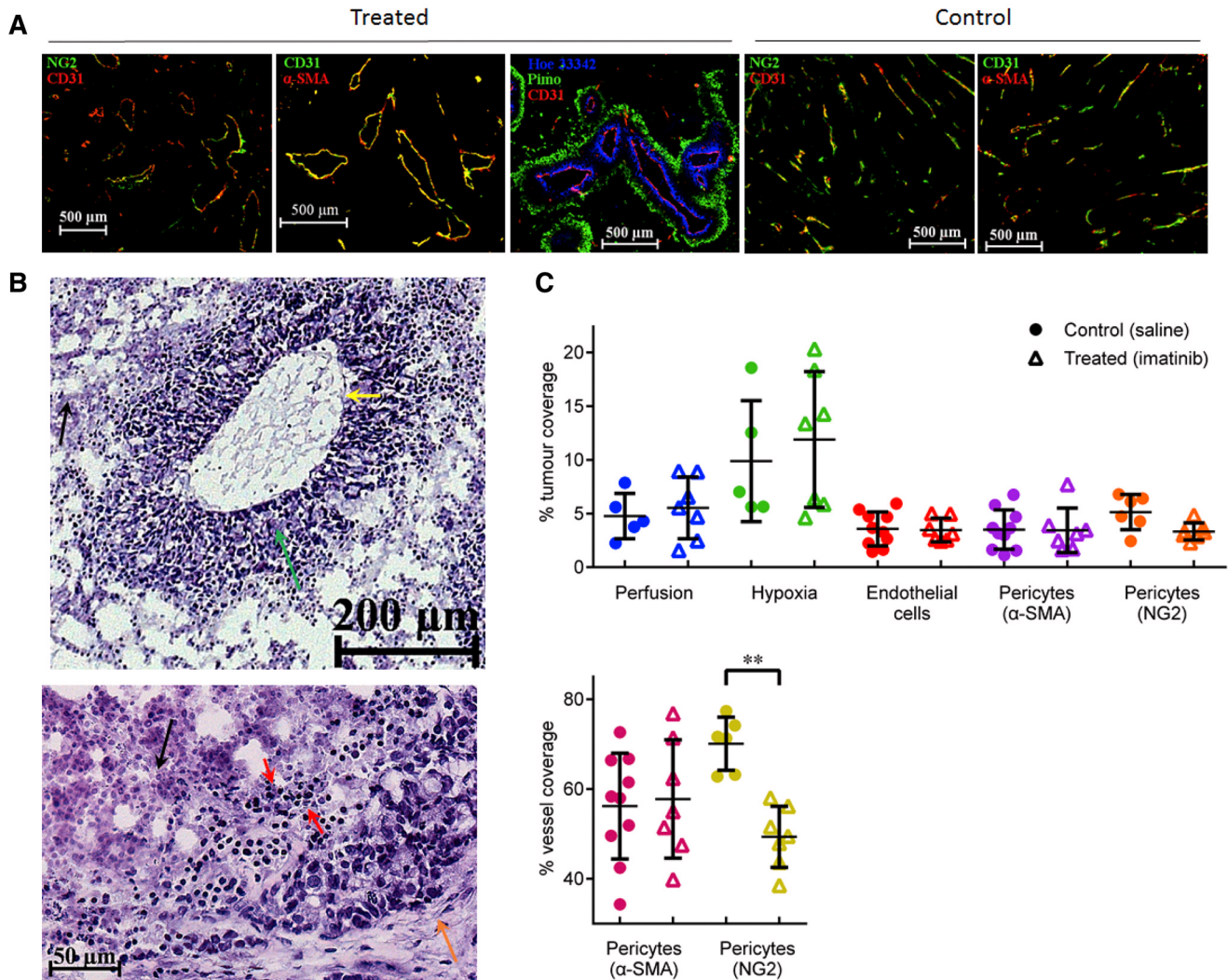


**Figure 6. Representative fluorescence microscopy images from imatinib-treated and control LS174T tumours. A)** Fluorescence microscopy images showing enlarged capillaries in treated but not in control tumours. **B)** H&E images showing regions of necrosis (black arrows), small and sparse round nuclei (red arrows, possibly revealing apoptosis) and viable tissue (green arrow) around capillaries (yellow arrow) or the tumour edge (orange arrow). **C)** Quantitative fluorescence microscopy results from control and treated LS174T tumours (day 5), showing the percentage tumour staining for perfusion, hypoxia, endothelial cells and pericytes (stained with either anti- $\alpha$ -SMA or anti-NG2 antibodies), and the percentage of blood vessels covered with pericytes. Error bars represent mean  $\pm$  SD. Imatinib treatment caused a significant decrease in the capillary coverage of pericytes stained with anti-NG2 but not with anti- $\alpha$ -SMA. Significance between distributions of treated and control tumours was assessed with a Mann-Whitney U-test. \*\*  $P < 0.01$ .

were significantly correlated. The cause of this disparity is unclear, but could be due in part to differences between preclinical and clinical MRI field strengths (9.4T vs 3T, respectively), or between tumour types.

### Conclusion

This study used BOLD and OE-MRI to assess the effect of the vascular-targeting therapeutic imatinib mesylate on cycling fluctuations in tumour oxygenation, vascular responsiveness to inhaled gas challenges, and chronic hypoxia. No evidence of vascular

normalisation was observed following 5 consecutive days of treatment in colorectal tumour xenograft models and, consequently, it could not be determined whether normalisation impacts on the amplitude or prevalence of cyclical fluctuations (which remained unchanged throughout). No change in OE-MRI measures were found, although the BOLD response to carbogen became significantly more positive in some tumour regions and more negative in other regions, thereby increasing overall heterogeneity. Whether this effect is linked to pericyte detachment requires further investigation.

## Data availability

Raw data generated from this study can be found at <http://doi.org/10.17605/OSF.IO/U6YTG49>

## Author contributions

Conception and design: MRG and SW-S. Development of methodology: MRG and SW-S. Acquisition of data: MRG. Analysis and interpretation of data: MRG and SW-S. Writing, review and/or revision of the manuscript: MRG, SPJ, RR, RBP, MFL and SW-S. Technical support (e.g. cell and animal work, image processing): MRG, SPJ and RR. Study supervision: SW-S.

## Competing interests

No competing interests were disclosed.

## Grant information

This work was carried out as part of King's College London and UCL Comprehensive Cancer Imaging Centre, and The Institute of Cancer Research Cancer Imaging Centre, CR-UK & EPSRC, in association with the Medical Research Council (MRC), Department of Health and British Heart Foundation (England) (C1519/A10331, C1519/A16463). RBP receives funding from the Medical Research Funding DPFS grant (MRC G100149). MFL receives funding from MRC (MR/J013110/1); the National Centre for the Replacement, Reduction and Refinement of Animal in Research (NC3Rs); UK Regenerative Medicine Platform Safety Hub (MRC: MR/K026739/1). SW-S is a Wellcome Trust Senior Research Fellow (WT100247MA).

*The funders had no role in study design, data collection and analysis, decision to publish, or preparation of the manuscript.*

## References

- Robinson SP, Rijken PF, Howe FA, *et al.*: **Tumor vascular architecture and function evaluated by non-invasive susceptibility MRI methods and immunohistochemistry.** *J Magn Reson Imaging.* 2003; **17**(4): 445–54. [PubMed Abstract](#) | [Publisher Full Text](#)
- Burrell JS, Walker-Samuel S, Baker LC, *et al.*: **Exploring  $\Delta R_2^*$  and  $\Delta R_1$  as imaging biomarkers of tumor oxygenation.** *J Magn Reson Imaging.* 2013; **38**(2): 429–34. [PubMed Abstract](#) | [Publisher Full Text](#)
- O'Connor JP, Boulton JK, Jamin Y, *et al.*: **Oxygen-Enhanced MRI Accurately Identifies, Quantifies, and Maps Tumor Hypoxia in Preclinical Cancer Models.** *Cancer Res.* 2016; **76**(4): 787–95. [PubMed Abstract](#) | [Publisher Full Text](#) | [Free Full Text](#)
- Matsumoto S, Yasui H, Mitchell JB, *et al.*: **Imaging cycling tumor hypoxia.** *Cancer Res.* 2010; **70**(24): 10019–23. [PubMed Abstract](#) | [Publisher Full Text](#) | [Free Full Text](#)
- Dewhirst MW: **Relationships between cycling hypoxia, HIF-1, angiogenesis and oxidative stress.** *Radiat Res.* 2009; **172**(6): 653–65. [PubMed Abstract](#) | [Publisher Full Text](#) | [Free Full Text](#)
- Chaplin DJ, Olive PL, Durand RE: **Intermittent blood flow in a murine tumor: radiobiological effects.** *Cancer Res.* 1987; **47**(2): 597–601. [PubMed Abstract](#)
- Kimura H, Braun RD, Ong ET, *et al.*: **Fluctuations in red cell flux in tumor microvessels can lead to transient hypoxia and reoxygenation in tumor parenchyma.** *Cancer Res.* 1996; **56**(23): 5522–8. [PubMed Abstract](#)
- Lanzen J, Braun RD, Klitzman B, *et al.*: **Direct demonstration of instabilities in oxygen concentrations within the extravascular compartment of an experimental tumor.** *Cancer Res.* 2006; **66**(4): 2219–23. [PubMed Abstract](#) | [Publisher Full Text](#)
- Skala MC, Fontanella A, Hendargo H, *et al.*: **Combined hyperspectral and spectral domain optical coherence tomography microscope for noninvasive hemodynamic imaging.** *Opt Lett.* 2009; **34**(3): 289–91. [PubMed Abstract](#) | [Publisher Full Text](#) | [Free Full Text](#)
- Baudelet C, Ansiaux R, Jordan BF, *et al.*: **Physiological noise in murine solid tumours using T2\*-weighted gradient-echo imaging: a marker of tumour acute hypoxia?** *Phys Med Biol.* 2004; **49**(15): 3389–411. [PubMed Abstract](#) | [Publisher Full Text](#)
- Baudelet C, Cron GO, Ansiaux R, *et al.*: **The role of vessel maturation and vessel functionality in spontaneous fluctuations of T2\*-weighted GRE signal within tumors.** *NMR Biomed.* 2006; **19**(1): 69–76. [PubMed Abstract](#) | [Publisher Full Text](#)
- Brurberg KG, Benjaminsen IC, Dorum LM, *et al.*: **Fluctuations in tumor blood perfusion assessed by dynamic contrast-enhanced MRI.** *Magn Reson Med.* 2007; **58**(3): 473–81. [PubMed Abstract](#) | [Publisher Full Text](#)
- Nehmeh SA, Erdi YE: **Respiratory motion in positron emission tomography/computed tomography: a review.** *Semin Nucl Med.* 2008; **38**(3): 167–76. [PubMed Abstract](#) | [Publisher Full Text](#)
- Wang K, Yorke E, Nehmeh SA, *et al.*: **Modeling acute and chronic hypoxia using serial images of  $^{18}\text{F}$ -FMISO PET.** *Med Phys.* 2009; **36**(10): 4400–8. [PubMed Abstract](#) | [Publisher Full Text](#) | [Free Full Text](#)
- Michiels C, Tellier C, Feron O: **Cycling hypoxia: A key feature of the tumor microenvironment.** *Biochim Biophys Acta.* 2016; **1866**(1): 76–86. [PubMed Abstract](#) | [Publisher Full Text](#)
- Chou CW, Wang CC, Wu CP, *et al.*: **Tumor cycling hypoxia induces chemoresistance in glioblastoma multiforme by upregulating the expression and function of ABCB1.** *Neuro Oncol.* 2012; **14**(10): 1227–38. [PubMed Abstract](#) | [Publisher Full Text](#) | [Free Full Text](#)
- Dewhirst MW, Cao Y, Moeller B: **Cycling hypoxia and free radicals regulate angiogenesis and radiotherapy response.** *Nat Rev Cancer.* 2008; **8**(6): 425–37. [PubMed Abstract](#) | [Publisher Full Text](#) | [Free Full Text](#)
- Druker BJ, Lydon NB: **Lessons learned from the development of an abl tyrosine kinase inhibitor for chronic myelogenous leukemia.** *J Clin Invest.* 2000; **105**(1): 3–7. [PubMed Abstract](#) | [Publisher Full Text](#) | [Free Full Text](#)
- Buchdunger E, Cioffi CL, Law N, *et al.*: **Abl protein-tyrosine kinase inhibitor STI571 inhibits *in vitro* signal transduction mediated by c-kit and platelet-derived growth factor receptors.** *J Pharmacol Exp Ther.* 2000; **295**(1): 139–45. [PubMed Abstract](#)
- Buchdunger E, O'Reilly T, Wood J: **Pharmacology of imatinib (STI571).** *Eur J Cancer.* 2002; **38**(Suppl 5): S28–36. [PubMed Abstract](#) | [Publisher Full Text](#)
- Jain RK: **Normalizing tumor vasculature with anti-angiogenic therapy: a new paradigm for combination therapy.** *Nat Med.* 2001; **7**(9): 987–9. [PubMed Abstract](#) | [Publisher Full Text](#)
- Battegay EJ, Rupp J, Iruela-Arispe L, *et al.*: **PDGF-BB modulates endothelial proliferation and angiogenesis *in vitro* via PDGF beta-receptors.** *J Cell Biol.* 1994; **125**(4): 917–28. [PubMed Abstract](#) | [Publisher Full Text](#) | [Free Full Text](#)
- Nissen LJ, Cao R, Hedlund EM, *et al.*: **Angiogenic factors FGF2 and PDGF-BB synergistically promote murine tumor neovascularization and metastasis.** *J Clin Invest.* 2007; **117**(10): 2766–77. [PubMed Abstract](#) | [Publisher Full Text](#) | [Free Full Text](#)
- Sato N, Beitz JG, Kato J, *et al.*: **Platelet-derived growth factor indirectly stimulates angiogenesis *in vitro*.** *Am J Pathol.* 1993; **142**(4): 1119–30. [PubMed Abstract](#) | [Free Full Text](#)
- Xue Y, Lim S, Yang Y, *et al.*: **PDGF-BB modulates hematopoiesis and tumor angiogenesis by inducing erythropoietin production in stromal cells.** *Nat Med.* 2011; **18**(1): 100–10. [PubMed Abstract](#) | [Publisher Full Text](#)
- Rajkumar VS, Boxer G, Robson M, *et al.*: **A comparative study of PDGFR inhibition with imatinib on radiolabeled antibody targeting and clearance in two pathologically distinct models of colon adenocarcinoma.** *Tumour Biol.* 2012; **33**(6): 2019–29. [PubMed Abstract](#) | [Publisher Full Text](#)

27. Vlahovic G, Rabbani ZN, Herndon JE 2nd, *et al.*: **Treatment with Imatinib in NSCLC is associated with decrease of phosphorylated PDGFR-beta and VEGF expression, decrease in interstitial fluid pressure and improvement of oxygenation.** *Br J Cancer.* 2006; **95**(8): 1013–9.  
[PubMed Abstract](#) | [Publisher Full Text](#) | [Free Full Text](#)
28. Vlahovic G, Ponce AM, Rabbani Z, *et al.*: **Treatment with imatinib improves drug delivery and efficacy in NSCLC xenografts.** *Br J Cancer.* 2007; **97**(6): 735–40.  
[PubMed Abstract](#) | [Publisher Full Text](#) | [Free Full Text](#)
29. Yener U, Avsar T, Akgün E, *et al.*: **Assessment of antiangiogenic effect of imatinib mesylate on vestibular schwannoma tumors using *in vivo* corneal angiogenesis assay.** *J Neurosurg.* 2012; **117**(4): 697–704.  
[PubMed Abstract](#) | [Publisher Full Text](#)
30. Cooke VG, LeBleu VS, Keskin D, *et al.*: **Pericyte depletion results in hypoxia-associated epithelial-to-mesenchymal transition and metastasis mediated by met signaling pathway.** *Cancer cell.* 2012; **21**(1): 66–81.  
[PubMed Abstract](#) | [Publisher Full Text](#) | [Free Full Text](#)
31. Pietras K, Pahler J, Bergers G, *et al.*: **Functions of paracrine PDGF signaling in the proangiogenic tumor stroma revealed by pharmacological targeting.** *PLoS Med.* 2008; **5**(1): e19.  
[PubMed Abstract](#) | [Publisher Full Text](#) | [Free Full Text](#)
32. Baranowska-Kortylewicz J, Abe M, Pietras K, *et al.*: **Effect of platelet-derived growth factor receptor-beta inhibition with STI571 on radioimmunotherapy.** *Cancer Res.* 2005; **65**(17): 7824–31.  
[PubMed Abstract](#) | [Free Full Text](#)
33. Pietras K, Rubin K, Sjöblom T, *et al.*: **Inhibition of PDGF receptor signaling in tumor stroma enhances antitumor effect of chemotherapy.** *Cancer Res.* 2002; **62**(19): 5476–84.  
[PubMed Abstract](#)
34. Pietras K, Stumm M, Hubert M, *et al.*: **STI571 enhances the therapeutic index of epothilone B by a tumor-selective increase of drug uptake.** *Clin Cancer Res.* 2003; **9**(10 Pt 1): 3779–87.  
[PubMed Abstract](#)
35. O'Connor JP, Aboagye EO, Adams JE, *et al.*: **Imaging biomarker roadmap for cancer studies.** *Nat Rev Clin Oncol.* 2017; **14**(3): 169–86.  
[PubMed Abstract](#) | [Publisher Full Text](#) | [Free Full Text](#)
36. Gonçalves MR, Peter Johnson S, Ramasawmy R, *et al.*: **Decomposition of spontaneous fluctuations in tumour oxygenation using BOLD MRI and independent component analysis.** *Br J Cancer.* 2016; **114**(12): e13.  
[PubMed Abstract](#) | [Publisher Full Text](#) | [Free Full Text](#)
37. Workman P, Aboagye EO, Balkwill F, *et al.*: **Guidelines for the welfare and use of animals in cancer research.** *Br J Cancer.* 2010; **102**(11): 1555–77.  
[PubMed Abstract](#) | [Publisher Full Text](#) | [Free Full Text](#)
38. Walker-Samuel S, Orton M, McPhail LD, *et al.*: **Bayesian estimation of changes in transverse relaxation rates.** *Magn Reson Med.* 2010; **64**(3): 914–21.  
[PubMed Abstract](#) | [Publisher Full Text](#)
39. O'Connor JP, Naish JH, Parker GJ, *et al.*: **Preliminary study of oxygen-enhanced longitudinal relaxation in MRI: a potential novel biomarker of oxygenation changes in solid tumors.** *Int J Radiat Oncol Biol Phys.* 2009; **75**(4): 1209–15.  
[PubMed Abstract](#) | [Publisher Full Text](#)
40. Hall AP: **Review of the pericyte during angiogenesis and its role in cancer and diabetic retinopathy.** *Toxicol Pathol.* 2006; **34**(6): 763–75.  
[PubMed Abstract](#) | [Publisher Full Text](#)
41. Murfee WL, Skalak TC, Peirce SM: **Differential arterial/venous expression of NG2 proteoglycan in perivascular cells along microvessels: Identifying a venule-specific phenotype.** *Microcirculation.* 2005; **12**(2): 151–60.  
[PubMed Abstract](#) | [Publisher Full Text](#)
42. Song S, Ewald AJ, Stallcup W, *et al.*: **PDGFRbeta+ perivascular progenitor cells in tumours regulate pericyte differentiation and vascular survival.** *Nat Cell Biol.* 2005; **7**(9): 870–9.  
[PubMed Abstract](#) | [Publisher Full Text](#) | [Free Full Text](#)
43. le Coutre P, Mologni L, Cleris L, *et al.*: ***In vivo* eradication of human BCR/ABL-positive leukemia cells with an ABL kinase inhibitor.** *J Natl Cancer Inst.* 1999; **91**(2): 163–8.  
[PubMed Abstract](#) | [Publisher Full Text](#)
44. Gaengel K, Genové G, Armulik A, *et al.*: **Endothelial-mural cell signaling in vascular development and angiogenesis.** *Arterioscler Thromb Vasc Biol.* 2009; **29**(5): 630–8.  
[PubMed Abstract](#) | [Publisher Full Text](#)
45. Pietras K, Ostman A, Sjöquist M, *et al.*: **Inhibition of platelet-derived growth factor receptors reduces interstitial hypertension and increases transcapillary transport in tumors.** *Cancer Res.* 2001; **61**(7): 2929–34.  
[PubMed Abstract](#)
46. Fyles A, Milosevic M, Pintilie M, *et al.*: **Long-term performance of interstitial fluid pressure and hypoxia as prognostic factors in cervix cancer.** *Radiother Oncol.* 2006; **80**(2): 132–7.  
[PubMed Abstract](#) | [Publisher Full Text](#)
47. Gonçalves MR, Johnson SP, Ramasawmy R, *et al.*: **Decomposition of spontaneous fluctuations in tumour oxygenation using BOLD MRI and independent component analysis.** *Br J Cancer.* 2015; **113**(8): 1168–77.  
[PubMed Abstract](#) | [Publisher Full Text](#) | [Free Full Text](#)
48. O'Connor JP, Naish JH, Jackson A, *et al.*: **Comparison of normal tissue R<sub>2</sub> and R<sub>2</sub>\* modulation by oxygen and carbogen.** *Magn Reson Med.* 2009; **61**(1): 75–83.  
[PubMed Abstract](#) | [Publisher Full Text](#)
49. Walker-Samuel S: **Imatinib.** In: Framework OS, editor. *Open Science Framework.* 2017.  
[Publisher Full Text](#)

# Open Peer Review

Current Referee Status:



Version 1

Referee Report 30 June 2017

doi:[10.21956/wellcomeopenres.12657.r23298](https://doi.org/10.21956/wellcomeopenres.12657.r23298)



**Bernard Gallez**

Biomedical Magnetic Resonance (REMA), Louvain Drug Research Institute, Université catholique de Louvain, Brussels, Belgium

## Current knowledge on tumor cycling hypoxia. Positioning of the work.

The paper of MR Goncalves *et al* is an interesting piece of work dealing with the phenomenon of cycling or acute hypoxia in tumors. This phenomenon remains an enigma in cancer research. After its discovery (1) and studies on the factors responsible for this phenomenon (essentially, the fluctuation in red blood cells) (2), it has been postulated that fluctuating hypoxia may be responsible for tumor aggressiveness and resistance to treatments including radiation therapy or chemotherapy (3-4). However, the impact on human tumors still remains speculative.

To increase our knowledge on the impact of cycling tumor hypoxia in cancer therapy, there is a crucial need for developing non-invasive methods that can be translated into human patients. The first description of such a method using non-invasive imaging was described by Baudelet *et al* in 2004 using Blood Oxygen Level Dependent (BOLD) Magnetic Resonance Imaging (MRI) (5). The main advantages were the non-invasiveness of the technology, the use of an endogenous contrast, and the high spatial (0.5 mmx0.5mm pixel size) and temporal resolution (10 s per scan). She also described that a treatment combining carbogen and nicotinamide induced a significant decrease in the number of fluctuating voxels (5). Using BOLD-MRI, she studied the influence of vessel maturity on the occurrence of the phenomenon. For the purpose, she correlated maps of spontaneous fluctuations in flow/oxygen and maps vessel maturity using BOLD-MRI during sequential hypercapnia and hypercapnic hyperoxia challenges in fibrosarcomas (6). Goncalves *et al* also studied the relationship between cycling hypoxia and pathophysiological patterns, including vessel maturity (7).

It is worthwhile to state that other methods such as Dynamic Contrast Enhanced (DCE)-MRI (8) or <sup>18</sup>F-FMISO-PET (9) were also described to tackle this phenomenon, but with a lower spatial and time resolution, 15 min and 24 hours, for DCE-MRI and PET, respectively. Unfortunately, all these methods do not provide real pO<sub>2</sub> measurements, but rather reflect variations in local hemodynamic changes. Two MR methods were more recently described in order to map real pO<sub>2</sub> fluctuations occurring inside tumors: <sup>19</sup>F-MR relaxometry (10) and EPR oximetry (11). While these methods are powerful tools of investigation in pre-clinical models, it is unlikely that they will be used rapidly into the clinical arena on a broad scale. Overall, while the BOLD contrast depends on many factors (12), BOLD-MRI is currently one of the most promising method for translation into the clinic. Interestingly, a first report has just been published very recently with the demonstration of the occurrence of cycling hypoxia in patients with head and neck

squamous cell carcinoma (HNSCC) (13).

In addition to the availability of methods able to tackle the phenomenon over entire tumors, there is also a need for treatments that can modulate the occurrence of the spontaneous fluctuations in oxygenation. By correlating their effect on cycling hypoxia and treatment outcome, it could pave the way to designing rational innovative combined therapies. In this context, the strategy of authors to use a PDGFR antagonist was sound as it could potentially induce a change in proportion of vessel maturity and a transient normalization window of the vasculature. It is worth to cite the recent work of Matsumoto who used sunitinib for the same purpose and observed a decrease in the occurrence of cycling hypoxia as demonstrated by *in vivo* EPR (14).

Overall, the results presented in the publication can be considered as negative results as imatinib did not induce the expected change neither in flow/oxygen fluctuations nor vessel maturity as measured by MRI. Interestingly, only a change in pericytes (NG2 marker) was observed. Because the results were not conclusive, it is difficult to extrapolate if the strategy of normalization of the vasculature could have an impact on cycling hypoxia. However, the strategy, the methods used were sound and appropriate, and this report definitely deserves publication. Closing a door is as important than opening a door.

### Minor specific points

1. The broad context and challenges of mapping tumor acute hypoxia and linking could be expanded in the introduction (see previous description)
2. The methods are adequately described and well performed. The rationale for using hypercapnia and hypercapnic hyperoxia could be a little bit more expanded for facilitate the reading (see ref 6 and 15)
3. Are there any result for tumor R2\* response on day 3?

### References

1. Brown JM: Evidence for acutely hypoxic cells in mouse tumours, and a possible mechanism of reoxygenation. *Br J Radiol.* 1979; **52** (620): 650-6 [PubMed Abstract](#) | [Publisher Full Text](#)
2. Kimura H, Braun RD, Ong ET, Hsu R, Secomb TW, Papahadjopoulos D, Hong K, Dewhirst MW: Fluctuations in red cell flux in tumor microvessels can lead to transient hypoxia and reoxygenation in tumor parenchyma. *Cancer Res.* 1996; **56** (23): 5522-8 [PubMed Abstract](#)
3. Dewhirst MW, Cao Y, Moeller B: Cycling hypoxia and free radicals regulate angiogenesis and radiotherapy response. *Nat Rev Cancer.* 2008; **8** (6): 425-37 [PubMed Abstract](#) | [Publisher Full Text](#)
4. Michiels C, Tellier C, Feron O: Cycling hypoxia: A key feature of the tumor microenvironment. *Biochim Biophys Acta.* **1866** (1): 76-86 [PubMed Abstract](#) | [Publisher Full Text](#)
5. Baudelet C, Ansiaux R, Jordan BF, Havaux X, Macq B, Gallez B: Physiological noise in murine solid tumours using T2\*-weighted gradient-echo imaging: a marker of tumour acute hypoxia?. *Phys Med Biol.* 2004; **49** (15): 3389-411 [PubMed Abstract](#)
6. Baudelet C, Cron GO, Ansiaux R, Crockart N, DeWever J, Feron O, Gallez B: The role of vessel maturation and vessel functionality in spontaneous fluctuations of T2\*-weighted GRE signal within tumors. *NMR Biomed.* 2006; **19** (1): 69-76 [PubMed Abstract](#) | [Publisher Full Text](#)
7. Gonçalves MR, Johnson SP, Ramasawmy R, Pedley RB, Lythgoe MF, Walker-Samuel S: Decomposition of spontaneous fluctuations in tumour oxygenation using BOLD MRI and independent component analysis. *Br J Cancer.* 2015; **113** (8): 1168-77 [PubMed Abstract](#) | [Publisher Full Text](#)

8. Brurberg KG, Gaustad JV, Mollatt CS, Rofstad EK: Temporal heterogeneity in blood supply in human tumor xenografts. *Neoplasia*. 2008; **10** (7): 727-35 [PubMed Abstract](#)
9. Wang K, Yorke E, Nehmeh SA, Humm JL, Ling CC: Modeling acute and chronic hypoxia using serial images of F18-FMISO PET. *Med Phys*. 2009; **36** (10): 4400-4408 [PubMed Abstract](#) | [Publisher Full Text](#)
10. Magat J, Jordan BF, Cron GO, Gallez B: Noninvasive mapping of spontaneous fluctuations in tumor oxygenation using F19 MRI. *Med Phys*. 2010; **37** (10): 5434-5441 [PubMed Abstract](#) | [Publisher Full Text](#)
11. Yasui H, Matsumoto S, Devasahayam N, Munasinghe JP, Choudhuri R, Saito K, Subramanian S, Mitchell JB, Krishna MC: Low-field magnetic resonance imaging to visualize chronic and cycling hypoxia in tumor-bearing mice. *Cancer Res*. 2010; **70** (16): 6427-36 [PubMed Abstract](#) | [Publisher Full Text](#)
12. Baudelet C, Gallez B: Current issues in the utility of blood oxygen level dependent MRI for the assessment of modulations in tumor oxygenation. *Current Medical Imaging Reviews*. 2005; **1** (3): 229-243
13. Panek R, Welsh L, Baker LCJ, Schmidt MA, Wong KH, Riddell AM, Koh DM, Dunlop A, Mcquaid D, d'Arcy JA, Bhide SA, Harrington KJ, Nutting CM, Hopkinson G, Richardson C, Box C, Eccles SA, Leach MO, Robinson SP, Newbold KL: Noninvasive Imaging of Cycling Hypoxia in Head and Neck Cancer Using Intrinsic Susceptibility MRI. *Clin Cancer Res*. 2017. [PubMed Abstract](#) | [Publisher Full Text](#)
14. Matsumoto S, Batra S, Saito K, Yasui H, Choudhuri R, Gadisetti C, Subramanian S, Devasahayam N, Munasinghe JP, Mitchell JB, Krishna MC: Antiangiogenic agent sunitinib transiently increases tumor oxygenation and suppresses cycling hypoxia. *Cancer Res*. 2011; **71** (20): 6350-9 [PubMed Abstract](#) | [Publisher Full Text](#)
15. Gilad AA, Israely T, Dafni H, Meir G, Cohen B, Neeman M: Functional and molecular mapping of uncoupling between vascular permeability and loss of vascular maturation in ovarian carcinoma xenografts: the role of stroma cells in tumor angiogenesis. *Int J Cancer*. 2005; **117** (2): 202-11 [PubMed Abstract](#) | [Publisher Full Text](#)

**Is the work clearly and accurately presented and does it cite the current literature?**

Partly

**Is the study design appropriate and is the work technically sound?**

Yes

**Are sufficient details of methods and analysis provided to allow replication by others?**

Yes

**If applicable, is the statistical analysis and its interpretation appropriate?**

Yes

**Are all the source data underlying the results available to ensure full reproducibility?**

Yes

**Are the conclusions drawn adequately supported by the results?**

Yes

**Competing Interests:** No competing interests were disclosed.

**Referee Expertise:** Tumor hypoxia, MRI, oximetry, cycling hypoxia, EPR, tumor hemodynamics, tumor metabolism

**I have read this submission. I believe that I have an appropriate level of expertise to confirm that it is of an acceptable scientific standard.**

Referee Report 19 June 2017

doi:[10.21956/wellcomeopenres.12657.r23297](https://doi.org/10.21956/wellcomeopenres.12657.r23297)



**Mark W. Dewhirst**<sup>1</sup>, **Xiaojie Zhang**<sup>2</sup>, **Ashlyn Rickard**<sup>3</sup>

<sup>1</sup> Duke Cancer Institute, Duke University, Durham, NC, USA

<sup>2</sup> Duke University School of Medicine, Duke University, Durham, NC, USA

<sup>3</sup> Duke Medical Physics, Duke University, Durham, NC, USA

### General Remarks:

Cycling (acute) hypoxia in tumors was first described in classic work of Martin Brown (1) and later by David Chaplin and Ralph Durand (2). The prevailing paradigm from that early work was that this feature of oxygen transport was the result of temporary vascular stasis. Later, it was established that vascular stasis is not required for this effect. The predominant cause was the result of fluctuations in red cell flux in tumor microvessels (3). Many other published papers have characterized some of the features of this phenomenon, as reviewed (4-6). For example, Fourier transform analyses have revealed a complex cyclical behavior, with the most predominant frequency in the range of 2-3 cycles per hour (7). Although cycling hypoxia has not been reported in human tumors, to date, it has been observed in companion canine solid tumors (8). The magnitude of these fluctuations varies considerably between tumor types (7, 9). Despite the extensive work to characterize cycling hypoxia in pre-clinical models, the clinical significance of cycling hypoxia is unknown. Imaging methods that can capture this dynamic hold promise for being able to test the clinical significance of cycling hypoxia. The two MRI-based methods studied in this paper are clinically translatable.

Blood Oxygen Level Detection (BOLD) was the first technique used to study cycling hypoxia, *in vivo* (10). More recently, Oxygen Enhanced (OE-MRI) has been reported to reflect tumor hypoxia, but to date studies using it to measure cycling hypoxia have not been reported (11). The BOLD signal is sensitive to the concentration of deoxyhemoglobin present in the blood (10), whereas the OE-MRI method is dependent upon the amount of oxygen that is dissolved in interstitial fluid (11). BOLD signal can be influenced by mitigating factors that are somewhat independent of the concentration of deoxyhemoglobin content of blood. These mitigating factors include changes in microvessel hematocrit and flow velocity (12). In contrast, OE-MRI is not subject to these potential errors. To date, however, a head-to-head comparison of these two methods in the same tumor type has not been reported. This particular paper uses both methods and the opportunity for a direct comparison exists. Unfortunately, however, this comparison was not made.

The majority of the studies of cycling hypoxia were done using point measurements of pO<sub>2</sub> (polarography or implantable fluorescence lifetime spectroscopy probes), which afford no insights into the potential underlying causes of these fluctuations. The fluctuations in red cell flux and hypoxia may be the product of instabilities in microvascular network flow dynamics, but to study this, one would have to be able to visualize the oxygen field throughout the entire tumor at multiple points in time. If one observes spatial relatedness in the fluctuations within the tumor, it is quite likely that network hemodynamics are contributing to cycling hypoxia. Relevant work to the issue of spatial coordination in oxygen instability has been done in window chambers, using phosphorescence lifetime imaging and with oxygen sensitive



nanoparticles (13, 14). However these tumors are very small and nearly two-dimensional. Whether spatial relatedness in cycling hypoxia extends to larger 3-dimensional tumors is unknown. One group has performed a semblance of this type of analysis using BOLD MRI (10), in orthotopically transplanted sarcomas of mice, but more work is required. There is a clear need for carefully performed studies using methods that can visualize an entire 3-dimensional tumor. The methods used in this paper are highly relevant to this issue, but analysis of spatial relatedness was not performed.

Another critical point that has not been resolved is whether cycling hypoxia occurs in deep-seated tumors. All of the measurements that have been done have been in peripheral tumors, either in mice or companion canine tumors. Laser Doppler measurements of variations in perfusion were conducted in human subjects, but these were also in superficial tumors (15). It is possible that cycling hypoxia occurs mainly in peripherally located tumors because fluctuation in muscle perfusion is part of the thermoregulatory process in mammals (16). The methods used in this paper could be used to examine this question, by focusing on deep-seated orthotopic tumors in pre-clinical models. If successful, such studies could be extended to human subjects.

The goals of this paper were to use BOLD and OE-MRI to study the dynamics of cycling and chronic hypoxia under baseline conditions, after treatment with imatinib and during carbogen breathing or breathing room air with 5% CO<sub>2</sub>. Using a nude mouse model with colorectal adenocarcinoma, the authors hypothesized that imatinib therapy, an inhibitor of platelet-derived growth factor, would decrease tumor hypoxia and cycling hypoxia by normalizing vasculature. Given the complexity of the manipulations made, it is difficult to come to an overall conclusion of whether this work adds to what is already known about cycling hypoxia. First, only one tumor model was studied and it was not studied in the orthotopic site. Given the variation in vascular maturity between different tumor types (17, 18), it is difficult to generalize the results to understand how the effects seen represent “typical” tumors.

The rationale for the choice of imatinib, a PDGFR antagonist, is not clearly defined. It has been shown previously that similar drugs reduce vascular density and pericyte coverage (19). Indeed this is what was seen here. So, the treatment of choice made the vasculature less mature. This is not consistent with the concept of vascular normalization. Furthermore, the relative timing of tumor growth, imatinib administration, imaging time relative to drug administration need to be detailed in the methods section.

From an analysis perspective, the authors examined the aggregate changes in individual voxels within the MRI tumor images, taking the cumulative fluctuations of all the voxels to be significant for changes in hypoxia. Given that hypoxia changes along both a spatial and temporal spectrum, to simply look at individual voxels yields only limited information. In comparable studies of cycling hypoxia using a mouse window chamber, watershed segmentation studies were performed examining not only individual pixels but also of neighboring pixels. This nearest-neighbor approach would allow structural information and patterns to be visualized across a given tumor (13). Furthermore, a Fourier analysis would be useful in studying the power fluctuations across k-space and how they relate to cycling hypoxia (7).

The work performed in this paper is technically sound. However, as written, the paper does not shed new light on cycling hypoxia, nor does it undertake further mechanistic explorations. As recommended above, additional analyses of the existing data could prove fruitful, however. It is strongly recommended that the authors consider a head to head comparison of BOLD vs. OE-MRI, under baseline conditions and in conditions following imatinib treatment. It is also strongly recommended that analysis of data sets for spatial relatedness could be quite fruitful. It is possible that the characteristics of spatial relatedness are affected by imatinib treatment, for example. It is recommended that the studies with the hyperoxic and hypercarbic gases be removed. These do not add anything meaningful to this work and carbogen is no

longer used clinically.

### Specific Comments:

#### 1. Abstract

The background explains the role of BOLD and OE-MRI well in the context of clinically-relevant tumor hypoxia studies; however, it requires an explanation of why hypoxia is clinically significant.

#### 2. Introduction

The introduction lays out clearly the aims of this study, and justifies well the usage of BOLD and OE-MRI to detect hypoxia cycling in solid tumors. In addition, the hypothesis, that imatinib as a vascular normalizing agent would reduce tumor hypoxia as well as the fluctuations of cycling hypoxia, is clearly written and easily understandable. However, in the selection of imatinib as the drug of choice, the authors lack a fuller explanation for why imatinib is chosen over other targeted agents, which more directly alter angiogenesis and tumor vasculature. Furthermore, justification of the gas challenge studies is necessary as it is unclear how they are significant to this study and how they are clinically relevant.

#### 3. Animal Models

The usage of nude mice for studying the human colorectal adenocarcinoma is appropriately selected. However, the sacrificing parameters, such as tumor threshold or a pre-selected time frame, need to be elucidated.

#### 4. Imatinib therapy protocol

The authors need to elaborate on the target/actual tumor volumes that marked the beginning of imatinib therapy.

#### 5. *In Vivo* MRI

The authors need to describe when the MRI imaging was performed in relation to the imatinib treatment that day. They indicate later in the paper that there are short half-life considerations, so the timescale is important to include.

In the third paragraph, it is unclear as to what this method will achieve. An intuitive understanding of the comparisons the authors will make is lacking based on the generic description. It needs to be made clear that the study is focusing on the comparison between carbogen and medical air, and medical air +5% CO<sub>2</sub> and medical air. Furthermore, the carbogen gas challenge induces vasoactive effects, and contributes to altered hematocrit independently of oxygen levels. As such, having a convoluted series of gas challenges, medical air vs carbogen, and medical air vs + medical air +5% CO<sub>2</sub>, simply adds greater noise to the study of cycling hypoxia changes induced by imatinib, and does not add new or useful information.

#### 6. MRI Data Analysis

The data analysis is well-explained and consistent between studies with an exception: if R1 is being defined in terms of 1/T1 (Equation 2), consistently define R2\* in that same manner. As for the methods of analysis, the authors chose a simplistic approach that does not take advantage of the subtleties of their data. A more robust approach of comparing groups of voxels and a Fourier analysis (as described earlier) would provide much needed originality and could yield more significant results. As it is, the figures that the authors' current analysis produces are confusing and nearly indecipherable.

#### 7. Histological Assessment

Immunohistochemical assessment and parameters, while not a perfect correlate to cycling hypoxia, are well delineated and explained. The authors explain the rationale behind staining for endothelial cells, pericytes (and explains the selection of dual markers), hypoxia, and perfusion. How do these results relate to the imaging results?

#### 8. Assessment of Tumor Growth Rate

The description and dual-measurements (using MRI and calipers) is well-described and succinct. However, a figure of the tumor volumes without normalization is needed.

#### 9. Effect of imatinib on BOLD MRI measurements of cycling hypoxia

The authors provided a thorough description of the results as well as the p-value to show a lack of significance.

Figures 2A and 2C show only one example voxel. It is unclear if this was representative of all the spontaneous voxel fluctuations.

In Figure 2C, the ordinate axes of the subfigures are reported differently making comparison impossible. Figures 2D and E need to be visualized differently as they are difficult to read with the majority of points overlapping. Although, as was suggested earlier, an analysis over multiple voxels would be more meaningful.

#### 10. BOLD MRI measurements during hyperoxia gas challenge

The results were well explained with a note on the implications of positive and negative  $\Delta R2^*$  values. As the authors go on to describe an interesting result, they fail to report the significance. Furthermore, the referenced Figures 3B, 3C and 3D are missing the data point for day 3. These data points either need to be included or replaced with an explanation describing a valid reason for excluding them.

#### 11. OE-MRI measurements

The method of comparing medical air and carbogen for evaluating tumor oxygenation is outdated and is not used in the clinic. Carbogen, as mentioned earlier, is also known to be vasoactive, which could affect the data significantly. This could also cause the discrepancy reported between this data and those previously published by O'Connor *et al.*

#### 12. Immunohistochemistry

The immunohistochemistry is not an adequate correlate of cycling hypoxia, given that cycling hypoxia is dynamic, time sensitive, and heterogeneous within the tumor. The immunohistochemistry only examines limited sections of tumors, and at one point in time.

#### 13. Effect of imatinib therapy on histological measures

Given the known therapeutic range of drug dosage as well as standardized regimen, the authors do well to address the discrepancy between the selected once daily regimen vs the conventional regimens (BID in other papers using Imatinib). The authors need to explain why the treatment window was shortened to 5 days. Furthermore, the challenge of the timing of the MRI scans with imatinib administration could be discussed further as to the reason why a BID or even more frequent regimen was not performed. Using sub-therapeutic doses could significantly impact data and limit the specific imatinib effect the authors attempt to study.

#### 14. Effect of imatinib therapy on spontaneous $R2^*$ fluctuations measured with BOLD MRI

This paragraph was repeated.

"However, even with confirmed pericyte detachment observed following therapy, spontaneous  $R2^*$  fluctuations were still present. This suggests that pericytes have a minor role in the production of

spontaneous fluctuations. Indeed, other studies have suggested that raised interstitial fluid pressure is responsible for the phenomenon, which can be caused by the periodic occlusion of vessels or systemic fluctuations in blood flow."

The point stated here does not add new information. Pericytes aid the contractile function of blood vessels. Furthermore, cycling hypoxia cannot be attributed to interstitial fluid pressure, which describes the fluid pressure gradient between the extravascular and intravascular space. Because of the presence of microvascular pores, interstitial fluid pressure cannot collapse tumor vessels. Vascular collapse occurs as a result of tissue pressure. This comes from continued cell proliferation within a confined space or from dense matrix, which can push on tumor vessels and collapse them. The authors should look at the extensive works by Rakesh Jain and colleagues, who have studied this issue for many years.

#### 15. BOLD and OE-MRI measurements in response to hyperoxia and hyperapnea

"Vessel hyperdilation was evident in histological measures, and this increased blood volume could increase the tumor's capacity for oxygen transport, resulting in a more negative  $\Delta R_2^*$ . In turn, a greater response to the challenge could increase the potential for vascular steal effects from the nearby vasculature, causing a more positive  $\Delta R_2^*$ ."

There is a misunderstanding of vascular steal effects. A dilated blood vessel will steal the supply from smaller vessels, leading to a more negative  $\Delta R_2^*$  effect. Furthermore, tumor perfusion is regulated by arteriolar function upstream of the capillary bed found within tumors. A dilated capillary does not necessarily result in greater perfusion, as the authors claim.

The OE discussion does not seem adequate for this paper, as barely any comparisons between OE and BOLD MRI were addressed.

## References

1. Brown JM: Evidence for acutely hypoxic cells in mouse tumours, and a possible mechanism of reoxygenation. *Br J Radiol.* 1979; **52** (620): 650-6 [PubMed Abstract](#) | [Publisher Full Text](#)
2. Chaplin DJ, Durand RE, Olive PL: Acute hypoxia in tumors: implications for modifiers of radiation effects. *Int J Radiat Oncol Biol Phys.* 1986; **12** (8): 1279-82 [PubMed Abstract](#)
3. Kimura H, Braun RD, Ong ET, Hsu R, Secomb TW, Papahadjopoulos D, Hong K, Dewhirst MW: Fluctuations in red cell flux in tumor microvessels can lead to transient hypoxia and reoxygenation in tumor parenchyma. *Cancer Res.* 1996; **56** (23): 5522-8 [PubMed Abstract](#)
4. Dewhirst MW, Cao Y, Moeller B: Cycling hypoxia and free radicals regulate angiogenesis and radiotherapy response. *Nat Rev Cancer.* 2008; **8** (6): 425-37 [PubMed Abstract](#) | [Publisher Full Text](#)
5. Dewhirst MW: Relationships between cycling hypoxia, HIF-1, angiogenesis and oxidative stress. *Radiat Res.* 2009; **172** (6): 653-65 [PubMed Abstract](#) | [Publisher Full Text](#)
6. Bristow RG, Hill RP: Hypoxia and metabolism. Hypoxia, DNA repair and genetic instability. *Nat Rev Cancer.* 2008; **8** (3): 180-92 [PubMed Abstract](#) | [Publisher Full Text](#)
7. Braun RD, Lanzen JL, Dewhirst MW: Fourier analysis of fluctuations of oxygen tension and blood flow in R3230Ac tumors and muscle in rats. *Am J Physiol.* 1999; **277** (2 Pt 2): H551-68 [PubMed Abstract](#)
8. Brurberg KG, Skogmo HK, Graff BA, Olsen DR, Rofstad EK: Fluctuations in pO<sub>2</sub> in poorly and well-oxygenated spontaneous canine tumors before and during fractionated radiation therapy. *Radiother Oncol.* 2005; **77** (2): 220-6 [PubMed Abstract](#) | [Publisher Full Text](#)
9. Cárdenas-Navia LI, Yu D, Braun RD, Brizel DM, Secomb TW, Dewhirst MW: Tumor-dependent kinetics of partial pressure of oxygen fluctuations during air and oxygen breathing. *Cancer Res.* 2004; **64** (17): 6010-7 [PubMed Abstract](#) | [Publisher Full Text](#)
10. Baudalet C, Ansiaux R, Jordan BF, Havaux X, Macq B, Gallez B: Physiological noise in murine solid tumours using T2\*-weighted gradient-echo imaging: a marker of tumour acute hypoxia?. *Phys Med Biol.* 2004; **49** (15): 3389-411 [PubMed Abstract](#)
11. O'Connor JP, Boulton JK, Jamin Y, Babur M, Finegan KG, Williams KJ, Little RA, Jackson A, Parker GJ,

Reynolds AR, Waterton JC, Robinson SP: Oxygen-Enhanced MRI Accurately Identifies, Quantifies, and Maps Tumor Hypoxia in Preclinical Cancer Models. *Cancer Res.* 2016; **76** (4): 787-95 [PubMed Abstract](#) | [Publisher Full Text](#)

12. Neeman M, Dafni H, Bukhari O, Braun RD, Dewhirst MW: In vivo BOLD contrast MRI mapping of subcutaneous vascular function and maturation: validation by intravital microscopy. *Magn Reson Med.* 2001; **45** (5): 887-98 [PubMed Abstract](#)

13. Cárdenas-Navia LI, Mace D, Richardson RA, Wilson DF, Shan S, Dewhirst MW: The pervasive presence of fluctuating oxygenation in tumors. *Cancer Res.* 2008; **68** (14): 5812-9 [PubMed Abstract](#) | [Publisher Full Text](#)

14. Palmer GM, Fontanella AN, Zhang G, Hanna G, Fraser CL, Dewhirst MW: Optical imaging of tumor hypoxia dynamics. *J Biomed Opt.* **15** (6): 066021 [PubMed Abstract](#) | [Publisher Full Text](#)

15. Hill SA, Pigott KH, Saunders MI, Powell ME, Arnold S, Obeid A, Ward G, Leahy M, Hoskin PJ, Chaplin DJ: Microregional blood flow in murine and human tumours assessed using laser Doppler microprobes. *Br J Cancer Suppl.* 1996; **27**: S260-3 [PubMed Abstract](#)

16. Anderson GS: Human morphology and temperature regulation. *Int J Biometeorol.* 1999; **43** (3): 99-109 [PubMed Abstract](#)

17. Abramovitch R, Dafni H, Smouha E, Benjamin LE, Neeman M: In vivo prediction of vascular susceptibility to vascular susceptibility endothelial growth factor withdrawal: magnetic resonance imaging of C6 rat glioma in nude mice. *Cancer Res.* 1999; **59** (19): 5012-6 [PubMed Abstract](#)

18. Helfrich I, Scheffrahn I, Bartling S, Weis J, von Felbert V, Middleton M, Kato M, Ergün S, Augustin HG, Schadendorf D: Resistance to antiangiogenic therapy is directed by vascular phenotype, vessel stabilization, and maturation in malignant melanoma. *J Exp Med.* 2010; **207** (3): 491-503 [PubMed Abstract](#) | [Publisher Full Text](#)

19. Taylor TD, Hanna G, Yarmolenko PS, Dreher MR, Betof AS, Nixon AB, Spasojevic I, Dewhirst MW: Effect of pazopanib on tumor microenvironment and liposome delivery. *Mol Cancer Ther.* 2010; **9** (6): 1798-808 [PubMed Abstract](#) | [Publisher Full Text](#)

**Is the work clearly and accurately presented and does it cite the current literature?**

Partly

**Is the study design appropriate and is the work technically sound?**

Partly

**Are sufficient details of methods and analysis provided to allow replication by others?**

Partly

**If applicable, is the statistical analysis and its interpretation appropriate?**

Partly

**Are all the source data underlying the results available to ensure full reproducibility?**

No

**Are the conclusions drawn adequately supported by the results?**

No

**Competing Interests:** No competing interests were disclosed.

**Referee Expertise:** Tumor hypoxia, cycling hypoxia, drug transport, angiogenesis, hyperthermia, companion animal cancers

**We have read this submission. We believe that we have an appropriate level of expertise to confirm that it is of an acceptable scientific standard, however we have significant reservations, as outlined above.**

---